Journal of King Saud University – Engineering Sciences (2013) **25**, 75–80

King Saud University

Journal of King Saud University – Engineering Sciences

www.ksu.edu.sa
www.sciencedirect.com

ORIGINAL ARTICLE

Characterization of properties of Al–Al_2O_3 nano-composite synthesized via milling and subsequent casting

Mohsen Hossein-Zadeh [a], Mansour Razavi [b,*], Omid Mirzaee [a], Razieh Ghaderi [b]

[a] *Department of Materials Engineering, Semnan University, Semnan, Iran*
[b] *Materials and Energy Research Center, Tehran, Iran*

Received 18 October 2011; accepted 6 March 2012
Available online 12 March 2012

KEYWORDS

Mechanical activation;
Casting;
Mechanical properties;
Nano-composite

Abstract In this research, the feasibility of adding mechanically activated nano-crystalline Al_2O_3 particles into aluminum matrix was investigated. For this purpose, Al_2O_3 powder was milled in a high-energy ball mill for 20 h. Subsequently, 1 wt.% of Al_2O_3 powder was added to molten Al. Then microstructure, powder characterizations and mechanical and wear properties of this composite were studied. Peak broadening of the diffraction patterns clearly showed that Al_2O_3 crystallites were in the nanometer scale after milling. Furthermore, distributing a small amount of Al_2O_3 particles on the aluminum matrix was a heterogeneous feature and the grain size of the matrix consequently decreased. Due to the existence of hard particles and hence smaller crystalline size, hardness, yield strength and wear resistance of Al–Al_2O_3 composite significantly rised.

1. Introduction

Metal matrix composites (MMCs) receive great attention for many applications in aerospace, defense and automobile industries. These materials have been considered for use in automobile brake rotors and various components in internal combustion engines due to their high amount of strength to weight ratio (Razavi Hesabi et al., 2006; Woo and Lee, 2007). With regard to the prominence of aluminum metal matrix composites, a group of new advanced materials are significantly taken into account for their light weight, high strength, high specific modulus, low coefficient of thermal expansion and good wear resistance properties (Woo and Lee, 2007). In addition, high specific stiffness, superior high temperature, mechanical properties and excellent oxidation resistance of Al_2O_3 have developed a special class of these advanced materials i.e. Al–Al_2O_3 composites (Hassan and Gupta, 2008; Zebarjad and Sajjadi, 2007).

The production methods of such composites could be categorized into solid phase processes, liquid phase process and semi-solid fabrication process (Hoseini and Meratian, 2009). On the other hand, liquid processes possess several advantages including high production rate, low cost and the feasibility of producing complex parts (Hoseini and Meratian, 2009; Naji

* Corresponding author. Tel.: +98 261 6204131; fax: +98 261 6201888.
E-mail addresses: m7816006@yahoo.com, m-razavi@merc.ac.ir (M. Razavi).
Peer review under responsibility of King Saud University.

ELSEVIER Production and hosting by Elsevier

http://dx.doi.org/10.1016/j.jksues.2012.03.001

Table 1 The chemical composition of the Al ingot measurement by XRF.

Element	Al	Si	Fe	Cu	Mn	Mg	Zn	Ti	Ni
Weight percent	99.553	0.130	0.280	0.020	0.003	0.002	0.005	0.005	0.002

et al., 2008). However, the major problem for the production of these materials is to obtain the wetting of reinforcement by the liquid metal, which is very poor and is favored by strong chemistry bonding at the interface. The poor wetting is because of the presence of a film oxide at the surface of the aluminum. The wettability is a complex phenomenon that depends on the factors such as geometry of interface, process temperature, soaking time, and it determines the quality of bonding among the systems. Recently, ultrasonic dispersion of nano-scaled ceramic particles in the molten aluminum has been conducted in order to distribute the reinforcement particles throughout the matrix (Razavi Hesabi et al., 2006; Rajan et al., 2007). Also, various methods are applied to improve the wettability of Al_2O_3 particles in molten Al such as utilizing some alloying elements to the melt, wrapping the surface of the particles using CVD or PVD methods, making mechanical toss in the melt, applying force on the melt and controlling the atmosphere (Naji et al., 2008; Asavavisithchai and Kennedy, 2006; Yu et al., 2003; Olszówka-Myalska et al., 2003). Use of vortex mixing method is another alternative way to improve the wettability of these particles in contact with the molten metal.

There are some articles which investigated the role of effective parameters such as volume fraction and size distribution of particles during Al–Al_2O_3 composites' production via vortex process (Daoud and Reif, 2002; Mazahery et al., 2009; Yılmaz and Buytoz, 2001). But the influence of nano-crystalline Al_2O_3 as an ultra-fine reinforcement on the aluminum matrix has not been investigated in the researches extensively. In this study, nano-crystalline Al_2O_3 powders fabricated via milling process were distributed into an Al matrix to examine their impacts on mechanical and wear properties of this versatile composite.

2. Experiment

In this research raw materials involved: aluminum ingot with chemical composition visible in Table 1 as the composite's matrix, Al_2O_3 powder as reinforcement phase with the purity of $>99.99\%$ and mean particle size of 40 μm and at last a certain quantity of magnesium chips with purity of $>99\%$ and mean particle size of 2 mm was used in order to improve the degree of wettability of alumina particles within the molten aluminum. At first, Al_2O_3 powders were milled and refined by a high-energy planetary ball mill for 20 h within an alumina cup and with alumina balls. In order to raise the ball mill efficiency (according to our previous research Razavi et al., 2008), the rotation speed of disk and cup was chosen as 410 and 700 rpm, respectively. The balls to powder ratio were 10:1 and 5 balls with 20 mm in diameter were charged.

In casting step, an atmospheric control electrical furnace with the ultimate temperature of 1100 °C was applied. In order to protect materials against oxidation and other undesirable reactions during casting process, a pure argon gas has to be charged in an appropriate amount into the furnace. For this purpose and for removing more moisture and oxygen from the internal ambient of the furnace argon gas was passed through a silica gel column and tube furnace with a few copper chips at 300 °C with 5 l/min rate of flow for all runs was used. Melting temperature was determined by an optical pyrometer with the accuracy of ± 10 °C. All specimens were melted in an alumina crucible and cast in a cylindrical metallic mold made of iron with 25 mm in height and 9 mm in diameter. The temperature before casting was 800 °C and samples were removed from the mold after the cooling procedure. In order to compare the properties and structures of the samples, two aluminum ingots were melted in an identical condition (involve

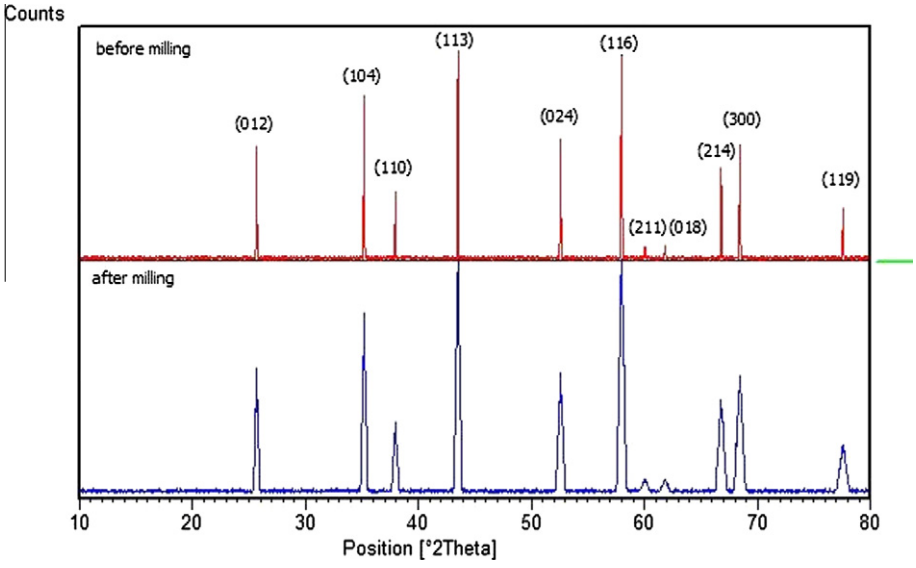

Figure 1 XRD patterns of Al_2O_3 powder before and after milling for 20 h.

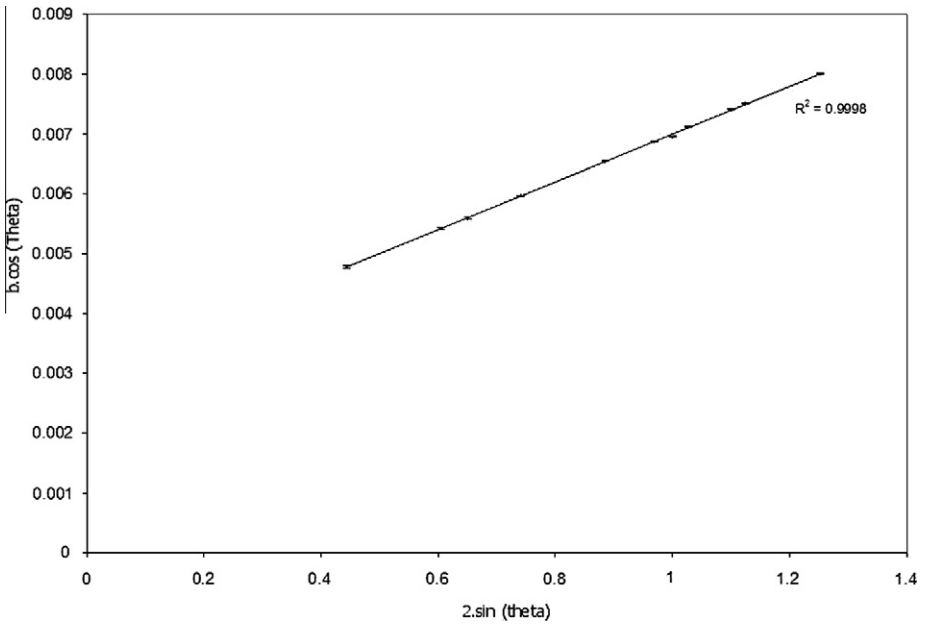

Figure 2 Williamson–Hall equation curve for determination of mean crystalline size and strain in milled samples.

Table 2 Crystallite size (d) and lattice strain (η) of the milled powder for 20 h (R^2: regression coefficient).

Milling time (h)	$b\cos\theta = \frac{0.9\lambda}{d} + 2\eta\sin\theta$		d (nm)	η (%)	R^2
	η	$0.9\lambda/d$			
20	0.004	0.0003	46	0.4	0.9998

casting temperature, furnace, crucible types, etc.), one of them was without any additives and the other contained 0.10 wt.% magnesium chips and 1.00 wt.% Al_2O_3 milled powder. Then, it was kept at the maximum temperature for 5 min after entering additives in the molten aluminum. During the process, a mechanical mixer was employed to develop a vortex flow through molten metal. Swirling speed of the mixer was maintained at 450 rpm steadily.

Afterward, the specimens were polished and etched. The etching solution contained 5, 10 and 85 cc of HCl, H_2SO_4 and distilled H_2O, respectively. A Philips XL30 Scanning Electron Microscopy (SEM) was utilized for morphological evaluations of the end-products before and during milling. X-ray diffraction analyses were conducted using a Bruker D8 X-ray diffractometer (Cu-Kα radiation, $\lambda = 1.54$) to determine formed phases and their crystallite size through Williamson–Hall method according to the $b\cos\theta = \frac{0.9\lambda}{d} + 2\eta\sin\theta$ equation (Razavi et al.,2007, 2008) (b, θ, λ, d and η are full-width of the peak at half of its maximum intensity, the Bragg angle, the wavelength of the X-ray used, average crystallite size and internal micro-strain in the powder, respectively). Also for the removal of instrument broadening, pure Al_2O_3 which was annealed at 800 °C for 5 h under argon gas has been used as a standard sample.

In tribological studies, pin-on-disk wear testing was performed with the final load 5 N, sliding distance of 400, 800 and 1200 m and sliding speed of 0.1 m/s according to ASTM: G99-95a (2000a). In this test, the cast sample was used as disk ($\varphi = 10$ mm) beside an alumina pin with mean hardness of

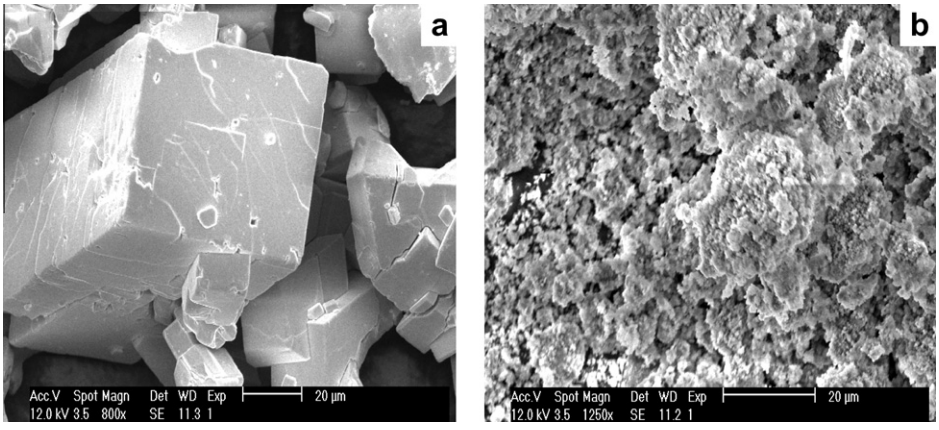

Figure 3 SEM micrograph of Al_2O_3 particles (a) before milling and (b) after milling.

Figure 4 OM image from Al–Al_2O_3 composite.

1600 ± 15 Vickers. The conditions of experiments were normal (normal atmosphere, temperature at the range of 18–22 °C and the humidity of 37–41%). The machine was stopped at certain distances and the weight losses of the samples were measured by an analytical balance with the accuracy of 0.0001 g. The samples were washed with acetone, vibrated by ultrasonic instrument and dried before being weighed. To determine the compressive strength, compression test was performed according to ASTM: E9-89a (2000b). The samples' diameter and height in the pressure test were 6 and 12 mm, respectively. Finally, to measure the hardness of the samples, Brinell method was used according to ASTM: E10 (2000c). All aforementioned tests were done 5 times and the averages of results were reported.

3. Results and discussion

The X-ray diffraction patterns of Al_2O_3 powders before and after 20 h milling are illustrated in Fig. 1. As it can be seen in this figure, milling process has not caused to create any new products so that Al_2O_3 with reference code of 001-1243 according to ICCD (The International Centre for Diffraction Data) was the only phase which was detected in the patterns. Activating powders by milling resulted in peak broadening and a slight decrease in the intensities that indicate a decline in the crystalline size of phases (Razavi et al., 2007).

The mean crystalline size of Al_2O_3 powder and the amount of internal stress created within the milled samples were determined by Williamson–Hall method that can be inferred from Fig. 2. The size of the crystals and the mean strain of the Al_2O_3 phase in milled system are presented in Table 2. As it is observable, crystallite size is in nanometer scale. High regression coefficient in Fig. 2 can be confirmed by these calculations. It is predicted that if the milling process continues, the grains will become finer until they reach a critical value. The rational reason for this prediction is that mechanical milling

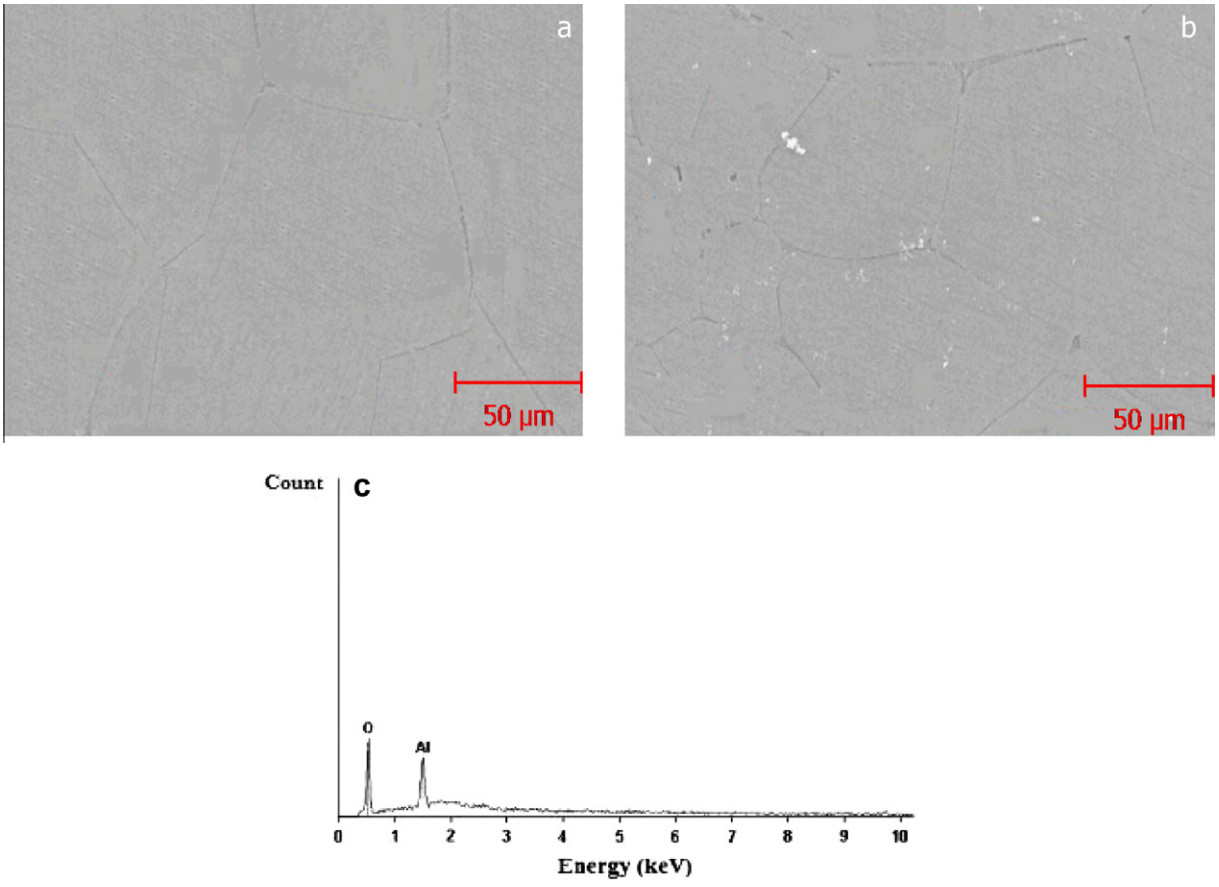

Figure 5 SEM micrograph of (a) pure aluminum, (b) Al–Al_2O_3 composite and (c) EDS from white particles in (b).

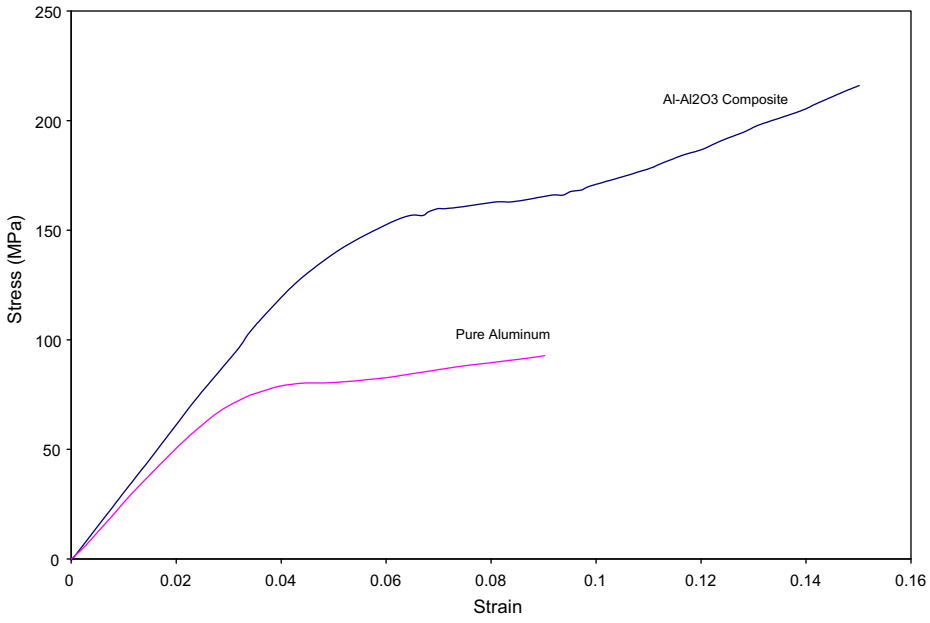

Figure 6 Stress vs. strain curve of Al–Al_2O_3 composite and Al without Al_2O_3.

is the result of the competition between cold fusions and breaking procedures of components that cause the fineness and the activation of particles. At the critical point, the speed of fusion and breaking will be balanced and the particles will no longer be fined (Razavi et al., 2007, 2008).

Fig. 3 shows the SEM micrographs of the samples before and after 20 h milling. From these SEM images, it is obvious that the above mentioned powders were fine and had formed some agglomerates. When powders are mechanically milled, the energy of milling deforms the particles and gets flattened shapes by a micro-forging process.

In the next stage, 1.0 wt.% milled Al_2O_3 powder was added to molten aluminum. Microstructure of this composite is shown in Fig. 4. Homogeneous distribution of reinforcement phase was clarified in this figure. The SEM image of samples in etch mode is illustrated in Fig. 5. Because of higher density of Al_2O_3 rather than Al, the Al_2O_3 particles have been brighter than matrix. EDS from these particles confirmed the mentioned claim. Also from SEM pictures and Clemex software, it is obvious that the mean grain size of composite sample is finer than pure aluminum sample (mean grain areas are 4892.8 ± 5 and 3344.3 ± 3 μm^2 for pure aluminum and composite, respectively) due to the existence of Al_2O_3 since inhomogeneity nucleation in the matrix leads to smaller grains.

The measurement hardness was 40 ± 1 and 62 ± 1 HV for pure aluminum and reinforced sample, respectively. Also according to stress vs. strain curve (Fig. 6), yield strength of pure aluminum and composite was 74 ± 2 and 144 ± 1 MPa,

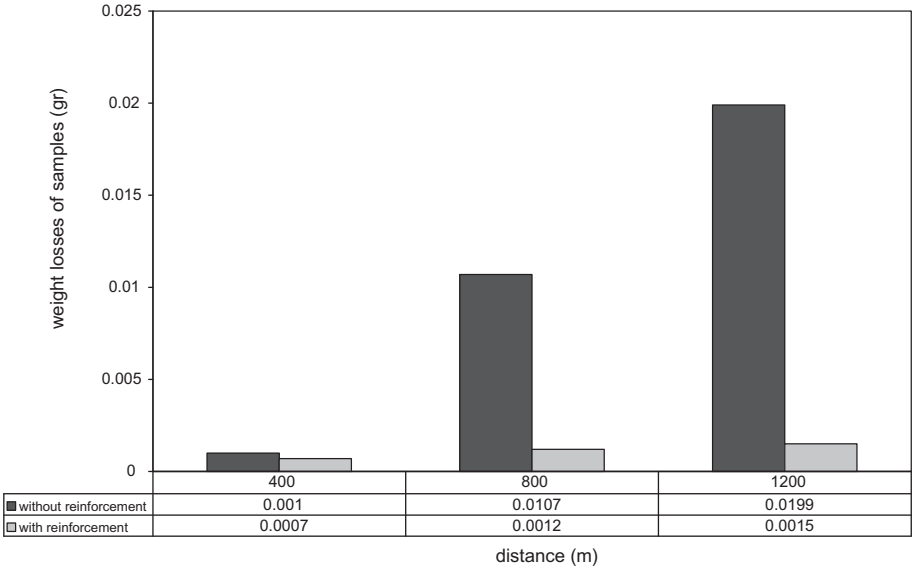

Figure 7 The weight losses of the samples vs. distance.

respectively. Improvement of mechanical properties can be attributed to two phenomena (Dieter and Bacon, 1986):

(1) *Strengthening from grain boundaries*: A general relationship between yield stress (and other mechanical properties) and grain size was proposed by Hall–Petch according to $\sigma_0 = \sigma_i + K{\cdot}D^{-1/2}$ equation (σ_0, σ_i, K and D are yield stress, friction stress, locking parameter and grain diameter, respectively). In this system, by adding Al_2O_3 to the molten aluminum its grains decreased and thereby its mechanical properties excessively rose.
(2) *Strengthening from fine particles*: Small second phase particles distributed in a ductile matrix are a common source of alloy strengthening. In this system, Al_2O_3 as fine particles throughout the matrix can act as barriers to the dislocations and thus mechanical properties were elevated.

Finally, the weight losses of the aluminum samples and the ones including 1 wt.% Al_2O_3 were measured via wear testing through the pin-on-disk method with the vertical force of 5 N in different distances. The results are shown in Fig. 7. It is noticeable that in short distance of 400 m, the weight losses of the two samples were the same, while as the wear distance increased, the weight losses drew significant differences so that the Al samples lost their weights 8.92 and 13.267 times greater than that of Al–1%Al_2O_3 composite in the distances of 800 and 1200 m, respectively. The above observations are very magnificent taking into account (with respect to) the small amount of the added Al_2O_3 to the melt and show the meaningful effect of this material on the wear properties of Al matrix. During dry sliding, the hard Al_2O_3 particles do not easily come out in the debris because of their reasonably good bonding with the matrix. Also according to Archard equation, due to higher hardness of composite sample, the wear resistance of Al–Al_2O_3 composite is better than pure aluminum too (Yang, 2003).

4. Conclusion

1. The crystallite size of the milled Al_2O_3 was in the scale of nanometer.
2. Al–Al_2O_3 composite with good distribution of second phase was produced successfully by adding nano-crystalline alumina to molten aluminum.
3. Microstructure of this composite is finer than pure aluminum due to the existence of fine alumina particles as heterogeneous nucleation.
4. Due to crystalline size reduction and existence of hard particles in matrix, mechanical properties (yield strain and hardness) of Al–Al_2O_3 composite were better than that of the sample without Al_2O_3.
5. Addition of small amounts of synthesized nano-crystalline Al_2O_3 powders to Al matrix could decrease the wear extent from 0.0199 to 0.0015 g in the wear distance of 1200 m.

References

Asavavisithchai, S., Kennedy, A.R., 2006. The effect of Mg addition on the stability of Al–Al_2O_3 foams made by a powder metallurgy route. Scripta Mater. 54, 1331–1334.

ASTM Designation: G99-95a, e1, 2000a. Standard test method for wear testing with a pin-on-disk apparatus.

ASTM Designation: E9-89a, e1, 2000b. Standard test methods of compression testing of metallic materials at room temperature.

ASTM Designation: E10, e1, 2000c. Standard test method for Brinell hardness of metallic materials.

Daoud, A., Reif, W., 2002. Influence of Al2O3 particulate on the aging response of A356 Al-based composites. J. Mater. Process. Technol. 123, 313–318.

Dieter, G.E., Bacon, D., 1986. Mechanical Metallurgy. McGraw-Hill, London.

Hassan, S.F., Gupta, M., 2008. Effect of submicron size Al_2O_3 particulates on microstructural and tensile properties of elemental Mg. J. Alloys Compd. 457, 244–250.

Hoseini, M., Meratian, M., 2009. Fabrication of in situ aluminum–alumina composite with glass powder. J. Alloys Compd. 471, 378–382.

Mazahery, A., Abdizadeh, H., Baharvandi, H.R., 2009. Development of high-performance A356/nano-Al_2O_3 composites. Mater. Sci. Eng., A 518, 61–64.

Naji, H., Zebarjao, S.M., Sajjadi, S.A., 2008. The effects of volume percent and aspect ratio of carbon fiber on fracture toughness of reinforced aluminum matrix composites. Mater. Sci. Eng., A 486, 413–420.

Olszówka-Myalska, A., Szala, J., leziona, J., Formanek, B., Myalski, J., 2003. Influence of Al–Al_2O_3 composite powder on the matrix microstructure in composite casts. Mater. Charact. 49, 165–169.

Rajan, T.P.D., Narayan Prabhu, K., Pillai, R.M., Pai, B.C., 2007. Solidification and casting/mould interfacial heat transfer characteristics of aluminum matrix composites. Compos. Sci. Technol. 67, 70–78.

Razavi, M., Rahimipour, M.R., Rajabi Zamani, A.H., 2007. Synthesis of nanocrystalline TiC powder from impure Ti chips via mechanical alloying. J. Alloys Compd. 436, 142–145.

Razavi, M., Rahimipour, M.R., Mansoori, R., 2008. Synthesis of TiC–Al_2O_3 nanocomposite powder from impure Ti chips, Al and carbon black by mechanical alloying. J. Alloys Compd. 450, 463–467.

Razavi Hesabi, Z., Simchi, A., Seyed Reihani, S.M., 2006. Structural evolution during mechanical milling of nanometric and micrometric Al_2O_3 reinforced Al matrix composites. Mater. Sci. Eng., A 428, 159–168.

Woo, K., Lee, H.B., 2007. Fabrication of Al alloy matrix composite reinforced with subsieve-sized Al_2O_3 particles by the in situ displacement reaction using high-energy ball-milled powder. Mater. Sci. Eng., A 449–451, 829–832.

Yang, L., 2003. Wear coefficient equation for aluminum-based matrix composites against steel disc. Wear 255, 579–592.

Yılmaz, O., Buytoz, S., 2001. Abrasive wear of Al_2O_3-reinforced aluminium-based MMCs. Compos. Sci. Technol. 61, 2381–2392.

Yu, Zh., Wu, G., Sun, D., Jiang, L., 2003. Coating of Y_2O_3 additive on Al_2O_3 powder and its effect on the wetting behaviour in the system Al_2O_3 p/Al. Mater. Lett. 57, 3111–3116.

Zebarjad, S.M., Sajjadi, S.A., 2007. Dependency of physical and mechanical properties of mechanical alloyed Al–Al_2O_3 composite on milling time. Mater. Des. 28, 2113–2120.